



Neutron capture cross-sections for ^{159}Tb isotope in the energy range of 5 to 17 MeV

B.K. Soni^a, Rajnikant Makwana^a, S. Mukherjee^{a,*}, Siddharth Parashari^a, S.V. Suryanarayana^b,
B.K. Nayak^b, H. Naik^c, M. Mehta^d

^a Department of Physics, Faculty of Science, The M. S. University of Baroda, Vadodra 390002, Gujarat, India

^b Nuclear Physics Division, Bhabha Atomic Research Centre, Mumbai 400085, India

^c Radiochemistry Division, Bhabha Atomic Research Centre, Mumbai 400085, India

^d Institute for Plasma Research, Gandhinagar, Gujarat 382428, India

HIGHLIGHTS

- Tb being an excellent structural metal has several reactor and nuclear medicines based applications.
- Tb isotopes are of keen interest of study since they are widely used in nuclear medicine.
- Calculations have been performed within the framework of theoretical code Talys-1.9.

ARTICLE INFO

Keywords:

$^{159}\text{Tb}(n, \gamma)^{160}\text{Tb}$ reaction

Covariance

γ -ray spectrometry

TALYS-1.9

Radiative capture

ABSTRACT

The neutron capture cross-sections have been measured for the $^{159}\text{Tb}(n, \gamma)^{160}\text{Tb}$ reaction at the spectrum average peak neutron energies of 5.08 ± 0.165 , 12.47 ± 0.825 , and 16.63 ± 0.95 MeV respectively. The experiment has been carried out using the standard neutron activation technique and off-line γ -ray spectrometry. The present measurement has been done for the energies where very few measured results are available in the data library. The results have been compared with ENDF/B-VII.1 and JENDL-4.0 data libraries. The present results have also been supported by theoretical predictions of nuclear model code TALYS 1.9. Detailed covariance analysis was carried out to find the uncertainty and the correlations among the measured cross-sections.

1. Introduction

Measurement of the neutron-induced reaction cross section of Terbium (Tb) is of great importance for the reactor technology and nuclear model development because it works as a venom in fission product. Terbium is commonly found as a rare-earth impurity in structural materials (Koning and Blomgren, 2009) and some isotopes which are widely used in nuclear medicine, like ^{149}Tb and ^{161}Tb are used in cancer treatment, ^{149}Tb and ^{152}Tb are used in Positron Emission Tomography (PET), while ^{155}Tb is used in Single Photon Emission Computed Tomography (SPECT). A nuclear reactor produces different high energy particles like α , β , γ and n during its operation. These particles irradiate the surrounding materials and produce radioactivity and hence damages the inside reactor core assembly. Therefore, the reaction cross section data for all these materials becomes vital for all possible neutron energies (Koning and Blomgren, 2009). On the other

hand, the knowledge of neutron capture cross-sections is also crucial for the design of the fast reactors and to improve the reactors which are currently in use. Hence, it is necessary to measure the experimental nuclear data in the neutron energy range from thermal to the maximum available neutron energies.

In the present work, we have measured the cross-section data for the $^{159}\text{Tb}(n, \gamma)^{160}\text{Tb}$ nuclear reaction for the incident particle energies of 5.08 ± 0.165 , 12.47 ± 0.825 , and 16.63 ± 0.95 MeV, respectively. The measured cross-sections have also been compared with the calculations done with the theoretical model code TALYS-1.9 (Koning et al., 2017). Different level density models have been tested for the best reproduction of the present and literature data (Dzysiuk et al., 2015; Voignier et al., 2017; Rigaud et al., 1971; Petö et al., 1967; Yunshan et al., 1988; Poenitz, 1982). Since the present work is based on relative measurement, therefore, the uncertainties in the measured cross-section were calculated by the covariance analysis (Shivashankar et al., 2015;

* Corresponding author.

E-mail address: sk.mukherjee-phy@msubaroda.ac.in (S. Mukherjee).

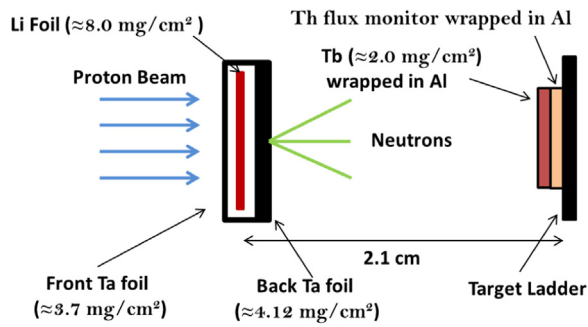


Fig. 1. Experimental arrangement of neutron irradiation which is generating from ${}^7\text{Li}(p, n)$ reaction.

Otuka et al., 2017). The covariance analysis enabled us to find the error and the relative correlation among the different quantities used in the present measurement.

2. Experimental technique

The experiment was performed at the Bhabha Atomic Research Center – Tata Institute of Fundamental Research (BARC-TIFR) Pelletron facility in Mumbai, India. The neutrons were produced by using the ${}^7\text{Li}(p, n)$ reaction using proton beams of 7.0, 15.0 and 18.8 MeV energies. The lithium (Li) foil of thickness 8.0 mg/cm^2 was encased with 3.7 mg/cm^2 Tantalum (Ta) from the front where the proton beam was targeted, and a thick Ta foil of thickness 4.12 mg/cm^2 from the backside to prevent the protons to interact with the ${}^{159}\text{Tb}$ sample. The degradation of protons in the first Ta foil was only 30 keV. On the other hand, the degradation in the back tantalum foil was sufficient to stop proton beam and allows only the neutrons to pass. The natural ${}^{159}\text{Tb}$ sample of thickness $\approx 2.0\text{ mg/cm}^2$ was placed at a distance of 2.1 cm from the lithium target to irradiate for about 5.0, 7.0, and 11.0 h with spectrum average peak neutron energies 5.08 ± 0.165 , 12.47 ± 0.825 , and $16.63 \pm 0.95\text{ MeV}$, respectively. The target assembly consisting of a sandwich of Ta-Li-Ta together with the ${}^{159}\text{Tb}$ target was placed inside the 6-meter irradiation port of the main beam line at TIFR pelletron. An experimental arrangement of the irradiation setup is shown in Fig. 1. The weight of the Tb foils was measured by using a digital microbalance weighing machine (Makwana et al., 2017) in order to calculate the number of target nuclei in each sample. The sample masses were found to be 32.2 (irradiation 1), 33.3 (irradiation 2) and 36.3 (irradiation 3) milligram respectively. In all the three irradiations, thorium (Th) foil was used as flux monitors (Makwana et al., 2017). After the accumulation of the radiation dose up to a safe limit, the irradiated samples of terbium were mounted on perspex plates and placed at a distance of 1 cm from the HPGe detector head for the gamma-ray spectrometry. The HPGe detector was pre-calibrated with a ${}^{152}\text{Eu}$ standard source and was connected to a PC based 4 K multichannel analyzer. The data analysis have been done by using the prominent gamma-ray of the residue, and other spectroscopic data as given in Table 1. In the present measurement, the product nuclide half-life, emission of prominent gamma-ray and isotopic abundances were taken from the NuDat (Rosman and Taylor, 1998; NNDC, 2017). A typical gamma ray spectrum obtained from the irradiated ${}^{159}\text{Tb}$ sample at $16.63 \pm 0.95\text{ MeV}$

Table 1
Spectroscopic data used in the present measurements.

| Reaction | Prominent γ -ray energy (KeV) | Branching Intensity (%) | Decay Mode (%) | Half-Life | Spin State J^π |
|---|--------------------------------------|-------------------------|----------------|-----------------------------|--------------------|
| ${}^{232}\text{Th}(n, f){}^{97}\text{Zr}$ | 743.360 ± 0.06 | 93.09 ± 0.01 | β -(100) | $16.749 \pm 0.008\text{ h}$ | $1/2^+$ |
| ${}^{159}\text{Tb}(n, \gamma){}^{160}\text{Tb}$ | 298.578 ± 0.17 | 26.1 ± 0.06 | β -(100) | $72.3 \pm 0.02\text{ d}$ | 3^- |
| | 879.378 ± 0.02 | 30.1 ± 0.06 | | | |
| | 1177.954 ± 0.03 | 14.9 ± 0.03 | | | |

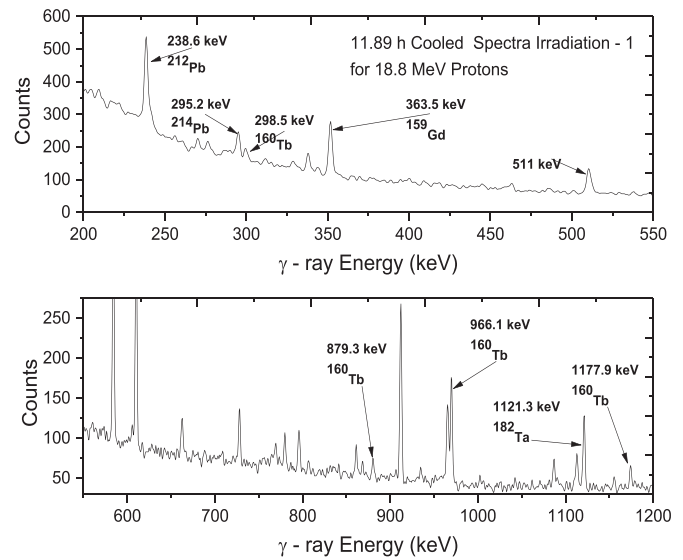


Fig. 2. Gamma ray spectrum from irradiated natural Tb isotope at $16.63 \pm 0.95\text{ MeV}$ neutron energy.

neutron energy is shown in Fig. 2.

3. Data analysis

3.1. Average neutron energy calculation

The neutrons were produced by the ${}^7\text{Li}(p, n)$ reaction. This reaction produce monoenergetic neutrons up to 2.4 MeV (Poppe et al., 1976). In the energy range 2.4 to 6 MeV, the first excited level of the isotope ${}^7\text{Be}$ at 0.43 MeV is populated and that generate the second group of neutrons. Above 6 MeV, three body interaction starts to contribute neutrons along with the main neutron group (Poppe et al., 1976; Anderson et al., 1970). All the produced neutrons from different reaction channel result into a quasi-mono energetic neutron spectrum. This consists of a main neutron peak and a long tail towards the lower side of the distribution. All these neutrons contribute to the production of reaction product. The measurement was performed at the main group of neutron spectrum average peak energy. The spectrum averaged neutron peak energy have been calculated by using the equation below (Smith, 2005; Makwana et al., 2017).

$$E_{\text{mean}} = \frac{\int_{E_{\text{ps}}}^{E_{\text{max}}} E_i \Phi_i dE}{\int_{E_{\text{ps}}}^{E_{\text{max}}} \Phi_i dE} \quad (1)$$

where: E_{max} = maximum neutron energy, E_{ps} = peak formation beginning for neutron energy, E_i = energy bin, Φ_i = neutron flux of E_i , E_{mean} = effective mean energy.

The neutron spectra were derived for 7.0, 15.0 and 18.8 MeV proton energies by using data from various available literature (Makwana et al., 2017). The neutron spectra for all the three incident energies are shown in Fig. 3. The calculated spectrum average peak energies for each distribution using Eq. (1) are presented in Table 2.

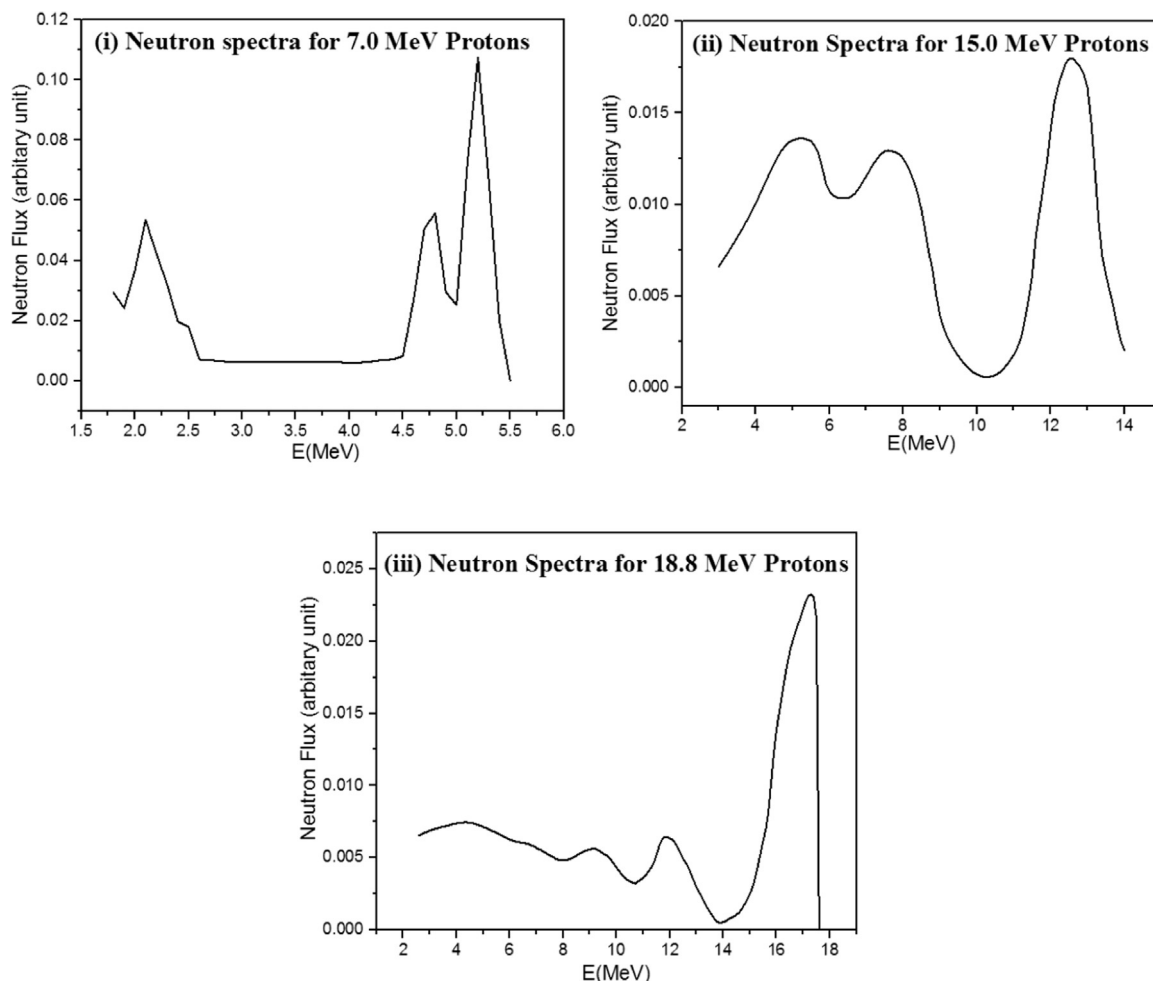


Fig. 3. (i) – (iii) Neutron spectra from ${}^7\text{Li}(p, n)$ reaction at proton energy (i) 7.0 MeV, (ii) 15.0 MeV and 18.8 (iii) MeV (Makwana et al., 2017).

Table 2
 ${}^{159}\text{Tb}(n, \gamma)$ reaction cross-section at different spectrum average peak neutron energies.

| Neutron Energy (MeV) | Cross-Section (mb) | | | |
|----------------------|-----------------------|--------------|-----------|-----------------------|
| | Measured | Tailing part | | Corrected |
| | | ENDF-B/VII.1 | JENDL-4.0 | |
| 16.63 ± 0.95 | 0.63061 ± 0.08253 | 0.01347 | 0.01016 | 0.61891 ± 0.08253 |
| 5.08 ± 0.165 | 1.00291 ± 0.12941 | 0.01106 | 0.00867 | 0.99311 ± 0.12941 |
| 12.47 ± 0.825 | 0.07490 ± 0.14540 | 0.07490 | 0.57440 | 1.28563 ± 0.14540 |

3.2. Neutron flux calculation

In order to estimate the cross-section, the accurate neutron flux calculation is essential. For the present experiment, ${}^{232}\text{Th}(n, f){}^{97}\text{Zr}$ monitor reaction was taken for the measurement of the neutron flux. The reaction product ${}^{97}\text{Zr}$ has a half-life of 16.749 ± 0.008 h (NNDC, 2017). The incident neutron flux calculation was carried out from the spectrum averaged neutron cross section for the monitor reaction by taking the recent relevant data from the ENDF/B-VII.1 (ENDF, 2018) data library for ${}^{232}\text{Th}(n, f)$ reaction (Jain et al., 1997; Garlea et al., 1992; Manabe et al.; 1998). It was calculated by using the Eq. (2) (Makwana et al., 2017).

$$\sigma_{av} = \frac{\int_{E_{th}}^{E_{max}} \sigma_i \Phi_i dE}{\int_{E_{th}}^{E_{max}} \Phi_i dE} \quad (2)$$

where: E_{max} = peak neutron energy, E_{th} = threshold energy of the monitor reaction, σ_i = cross-section at energy E_i for monitor reaction from ENDF (Lapenas, 1975; Loevestam et al., 2007; Agus et al., 2004; Uddin et al., 2013; Jain et al., 1997; Garlea et al., 1992; Manabe et al., 1988), Φ_i = neutron flux of energy bin E_i from Fig. 3(i)-(iii), σ_{av} = spectrum-averaged cross-section.

Following the method discussed above, the calculated spectrum averaged cross sections for the monitor reaction are given in Table 2. The spectrum averaged cross-sections were then used in Eq. (3) to calculate the incident neutron flux.

$$\Phi = \frac{A_\gamma \lambda (t_c / t_r)}{N_0 \sigma_{av} I_\gamma \varepsilon (1 - e^{-\lambda t_i})(1 - e^{-\lambda t_c}) e^{-\lambda t_w}} \quad (3)$$

where: N_0 = number of target atom, Φ = bombarded neutron flux ($n; \text{cm}^{-2}$), σ_{av} = spectrum averaged cross section, I_γ = branching intensity of gamma ray, ε = efficiency of detector related to chosen

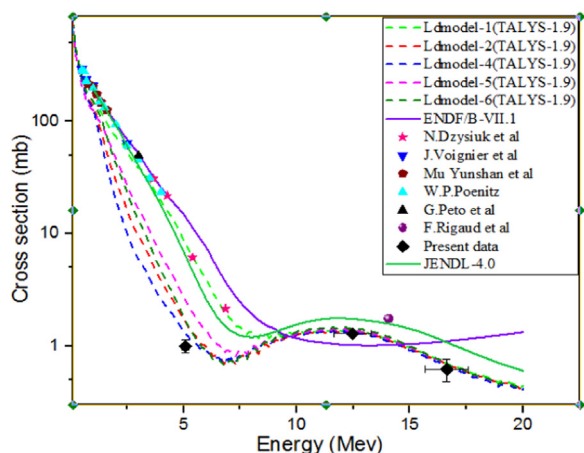


Fig. 4. Comparison of the experimentally measured $^{159}\text{Tb}(n,\gamma)^{160}\text{Tb}$ reaction cross section with literature data and the theoretical model codes values.

Table 3

Measured efficiencies with their correlation matrix.

| $E_\gamma(\text{KeV})$ | Efficiency | Correlation Matrix | | | |
|------------------------|-------------------------|--------------------|-------|---|--|
| 298.58 | 0.062016 ± 0.001242 | 1 | | | |
| 879.383 | 0.003587 ± 0.000193 | 0.069 | 1 | | |
| 1177.962 | 0.002584 ± 0.000088 | 0.373 | 0.861 | 1 | |

Table 4

Covariance matrix and corresponding Correlation matrix for the measured reaction cross-sections.

| $E_n(\text{MeV})$ | Covariance Matrix | | | Correlation Matrix | | |
|-------------------|-------------------|-------|--------|--------------------|-------|---|
| 16.63 ± 0.95 | 0.018 | | | 1 | | |
| 5.08 ± 0.165 | 0.004 | 0.017 | | 0.222 | 1 | |
| 12.47 ± 0.825 | 0.004 | 0.004 | 0.0128 | 0.261 | 0.269 | 1 |

gamma ray, t_r = clock time (s), t_c = counting time (s), t_w = cooling time (s), t_i = irradiation time (s), λ = decay constant of product nucleus (s^{-1}), A_γ = number of counts for detected gamma ray.

The measured values of the average neutron flux from the monitor reaction was used for estimation of the cross-section.

3.3. Neutron activation analysis

The experimental data were evaluated by using the standard neutron activation analysis (NAA) technique. This technique is based on the measurement of the reaction cross section by irradiating the target with neutrons. In this technique, the rate of creation of the product isotope depends on the nuclei available in the target and the incident neutron flux. This proportionality is given by the reaction cross section. The activated sample emits characteristic γ -rays having an adequately long half-life and γ branching abundances. By using the Eq. (4), the cross-section of the reaction can be calculated as,

$$\sigma = \frac{A_\gamma \lambda (t_c / t_r)}{N_0 \Phi I_\gamma \varepsilon (1 - e^{-\lambda t_c}) (1 - e^{-\lambda t_w}) e^{-\lambda t_w}} \quad (4)$$

where all the symbols have their meanings similar to Eq. (3).

In the Eq. (4), the peak area from the gamma spectrum was measured using MAESTRO spectroscopic software. The number of target nuclei (N_0) was calculated using the mass of each target. The neutron flux was calculated using the monitor reaction $^{232}\text{Th}(n, f)^{97}\text{Zr}$, which have been discussed in our previous publication (Makwana et al., 2017). Other standard parameters of the reactions were taken from the NuDat library (Rosman and Taylor, 1998; NNDC, 2017). Since quasi

mono-energetic neutron distribution were used in the present measurement, therefore, a contribution from the lower energy tail part comes into the measured cross-section. Hence, a correction has been taken into account to remove the lower energy tail part of the distribution. As suggested in literature (Makwana et al., 2017) the spectrum average reaction cross section was calculated for neutrons from lowest energy to peak start neutron energy. This was determined by taking convolution of neutron spectra and TALYS – 1.9 evaluated reaction cross section. This cross section has been subtracted from the present calculated reaction cross section. Thus the subtracted value gives the reaction cross section at the spectrum average neutron peak energy.

4. Theoretical analysis with TALYS-1.9

The theoretical calculations have been done to reproduce the measured cross-section by using a recent version of standard nuclear reaction modal code, TALYS 1.9 (Koning et al., 2017). The code is used extensively for nuclear data prediction for the emission of the gamma, neutron, proton, triton and other particles, by using the reaction parameter from the Reference Input Parameter Library (RIPL database) (Capote et al., 2009). The code deals with the effect of level density parameters on the compound nucleus, pre-equilibrium, and direct reaction mechanisms as a function of incident particle energy. Koning and Delaroche proposed the optical model parameters by using a global potential (Koning et al., 2017). By using the Hauser-Feshbach model, the compound reaction mechanism was incorporated (Hauserr and Feshbach, 1952). The pre-equilibrium contribution has been incorporated into the exciton model developed by Kalbach (1986). In the present work, the calculations have been done by considering all the parameter of the code as default like Deformation, Resonance, Gamma-ray, Optical model and Fission, and level density (LD) models. The comparison of theoretically predicted and EXFOR (2018) data with the present experimental results are shown in Fig. 4.

5. Results and discussion

In the present work, the final corrected $^{159}\text{Tb}(n, \gamma)^{160}\text{Tb}$ reaction cross sections at the spectrum average peak neutron energies of 5.08 ± 0.165 , 12.47 ± 0.825 , and 16.63 ± 0.95 MeV respectively, are given in Table 2 and plotted in Fig. 4. These cross sections are significant to improve the nuclear database and also crucial in the reactor design. For the validation of the present measured experimental data, the standard nuclear model plays a vital role. We can observe from Fig. 4 that, the reaction cross sections measured in the present work are in agreement with the predicted data using theoretical code TALYS 1.9 as well as with literature data (Dzysiuk et al., 2015; Voignier et al., 2017; Rigaud et al., 1971; Petö et al., 1967; Yunshan et al., 1988; Poenitz, 1982). Different level density models were tested for the reproduction of the present and the literature data from EXFOR (EXFOR, 2018). Among those, Ld model 1, which accounts for the constant temperature Fermi gas model (Gilbert and Cameron, 1965) have been found to be successful in the reproduction of cross-sections. However, the present data points were found consistent with the Ld model 4 predictions. The data were also compared with those from ENDF/B-VII.1 (2018) and JENDL-4.0 (2018) libraries. However, the present data at 5.08 ± 0.16 MeV is significantly lower than the literature data. It may also be observed that this cross section value agrees with data predicted by Ld model-4 of the theoretical code TALYS 1.9. It suggests that more experimental data are needed to be obtained and compared with the different nuclear models. Since the measured cross-sections are correlated with each other, therefore, a detailed covariance analysis have also been carried out in order to find out the exact values of the uncertainties in the measured data. Covariance analysis is a well-known method which can be used to calculate the uncertainty in the measured data by propagating the error in each quantity used in the

measurement. A discussion on the covariance analysis has been given in the following section.

6. Covariance analysis

In the present work, the reaction cross-sections were measured relative to the monitor reaction cross-section, and a common detector setup was used for recording of the spectra from each irradiated sample foil. Therefore, the measured cross-sections are correlated with the monitor reaction and with the efficiency of the detector used in the present measurement. The covariance analysis (Shivashankar et al., 2015; Otuka et al., 2017) utilizing a ratio method, (Otuka et al., 2017) which is the normalization of the measured cross-sections with respect to the monitor cross-sections, was used to find the correlation between the measured cross-sections from different correlating quantities. In this method, first we calculate the covariance and relative correlations among the efficiencies of the standard and the sample gamma lines. Then using the correlation factors, which came out from the first step, we deduce the covariance and the related correlation factors among the measured cross-sections. The calculated correlation coefficients for the efficiencies and measured cross section are shown in Tables 3, 4. The uncertainty in the measured cross-section calculated by taking the square root of diagonal elements of the covariance matrix and were found to be in the range of 11–14%, which are the optimum values for the present cross-section measurement consolidating the error from each of the quantity used in the calculations.

7. Summary

The experimental cross-sections for the $^{159}\text{Tb}(n, \gamma)^{160}\text{Tb}$ reaction were measured for the neutron energies of 5.08 ± 0.165 , 12.47 ± 0.825 , and 16.63 ± 0.95 MeV, respectively, by using the neutron activation analysis technique and including the standard tailing corrections (Poppe et al., 1976). The neutron flux measurement was done with the help of $^{232}\text{Th}(n, f)^{97}\text{Zr}$ monitor reaction. The uncertainty in the present measurement calculated with the help of covariance analysis was found to be in the range of 11–14%. All the measurements have been compared with the literature data (Dzysiuik et al., 2015; Voignier et al., 2017; Rigaud et al., 1971; Petö et al., 1967; Yunshan et al., 1988; Poenitz, 1982), ENDF/B-VII.1 (ENDF, 2018) JENDL-4.0 (2018) and the theoretical modular code TALYS 1.9 (Koning et al., 2017). The comparison of the present results show a good agreement with literature data as well as with ENDF/B-VII.1, JENDL-4.0 and TALYS-1.9 except for 5.08 ± 0.165 MeV, which was found lower compared to the theoretical predictions. The present work highlights that the nuclear reaction data can be measured within the uncertainty of $\approx 15\%$ by using the $^7\text{Li}(p, n)$ reaction as the quasi-monoenergetic neutron generator. The cross-section data presented in this work are essential for the data libraries, and for the future reactor technology.

Acknowledgments

One of the authors (SM) thanks the Department of Atomic Energy-Bhabha Atomic Research Centre (DAE-BRNS), Mumbai, India for the sanction of a major research project (Sanction Number: 36(6)/14/22/2016-BRNS). The authors are thankful to the staff of TIFR-BARC Pelletron facility for their kind cooperation and help to provide the proton beam to carry out the experiment. BKS is also thankful to Defense Research Development Organization (DRDO), India for the sanction of a major research project (DLJ/TC/1025/1/38) and to provide the funding for his research.

References

- Agus, Y., Celenk, I., Ozmen, A., 2004. Measurement of cross sections of threshold detectors with spectrum average technique. *Radiochim. Acta* 92, 63.
- Anderson, J.D., Wong, C., Madsen, V.A., 1970. Charge exchange part of the effective two-body interaction. *Phys. Rev. Lett.* 24, 1074.
- Capote, R., Herman, M., Obložinský, P., Young, P.G., Goriely, S., Belgya, T., Ignatyuk, A.V., Koning, A.J., Hilaire, S., Plujko, V.A., Avrigeanu, M., Bersillon, O., Chadwick, M.B., Fukahori, T., Zhigang, Ge, Han, Y., Kailas, S., Kopecky, J., Maslov, V.M., Reffo, G., Sin, M., Soukhovitskii, E.Sh, Talou, P., 2009. RIPL – reference input parameter library for calculation of nuclear reactions and nuclear data evaluations. *Nucl. Data Sheets* 110, 3107–3214.
- Dzysiuik, N., Kadenko, I., Gressier, V., Koning, A.J., 2015. Cross section measurement of the $^{159}\text{Tb}(n, \gamma)^{160}\text{Tb}$ nuclear reaction. *Nucl. Phys. A* 936, 6–16.
- ENDF/B-VII.1, 2018. National Nuclear Data Center, Brookhaven National Laboratory, <<https://www-nds.iaea.org/exfor/servlet/E4sMakeE4>>.
- EXFOR, 2018. Cross Section Information Storage and Retrieval System (EXFOR), IAEA, Vienna, Austria. <[http://www-nds.iaea.org/exfor/\(online\)](http://www-nds.iaea.org/exfor/(online))>.
- Garlea, I., Garlea, Chr, Rosu, H.N., Miron, Fodor, G., Raducu, V., 1992. Integral neutron cross sections measured around 14 MeV. *Rev. Roum. Phys.* 37, 19.
- Gilbert, A., Cameron, A.G.W., 1965. A composite nuclear-level density formula with shell corrections. *Can. J. Phys.* 43 (8), 1446–1496. <https://doi.org/10.1139/p65-139>.
- Hauser, W., Feshbach, H., 1952. The inelastic scattering of neutrons. *Phys. Rev.* 87, 366.
- Jain, R.K., Singh, H.V., Rao, J.R., Bose, S.K., 1997. Measurement of fast neutron induced fission cross section of thorium using Lexan plastic track detector. *Pramana* 49, 515.
- JENDL-4.0, <<https://www-nds.iaea.org/exfor/servlet/E4sMakeE4>>.
- Kalbach, C., 1986. Two-component exciton model: basic formalism away from shell closures. *Phys. Rev. C* 33, 818.
- Koning, A., Hilaire, S., Goriely, S., 2017. TALYS-1.9 - A Nuclear Reaction Program, User Manual, 1st ed. (NRG, Westerdinweg).
- Koning, A.J., Blomgren, J., 2009. Nuclear data for sustainable nuclear energy, JRC Scientific and Technical Report No. EUR23977EN-2009, retrieved from <https://cordis.europa.eu/pub/fp6-euratom/docs/candidefinal-report_en.pdf>.
- Lapenas, A.A., 1975. "Izmerenie Spektrov Neitronov Aktivacionym Metodom" Publishing House "ZINATNE", Riga, USSR (1975), (It contains an evaluation of 22 dosimetry reactions).
- Loevestam, G., Hult, M., Fessler, A., Gamboni, T., Gasparro, J., Jaime, R., Lindahl, P., Oberstedt, S., Tagziria, H., 2007. Measurement of neutron excitation functions using wide energy neutron beams. *Nucl. Instrum. Methods Phys. Res. Sect. A* 580, 1400.
- Makwana, Rajnikan, Mukherjee, S., Mishra, P., Naik, H., Singh, N.L., Mehta, M., Katovsky, K., Suryanarayana, S.V., Vansola, V., Santhi Sheela, Y., Karkera, M., Acharya, A., Khirwadkar, S., 2017. Measurement of the cross section of the $^{186}\text{W}(n, \gamma)^{187}\text{W}$, $^{182}\text{W}(n, p)^{182}\text{Ta}$, $^{154}\text{Gd}(n, 2n)^{153}\text{Gd}$, and $^{160}\text{Gd}(n, 2n)^{159}\text{Gd}$ reaction at neutron energies of 5 to 17 MeV. *Phys. Rev. C* 96, 02408.
- Manabe, F., Kanda, K., Iwasaki, T., Terayama, H., Karino, Y., Baba, M., Hirakawa, N., 1988. Measurements of neutron induced fission cross section ratios of ^{232}Th , ^{233}U , ^{234}U , ^{236}U , ^{238}U , ^{237}Np , ^{242}Pu and ^{243}Am Relative to ^{235}U around 14 MeV. *Fac. of Engineering, Tohoku Univ. Tech. Report* 52(Issue 2), p. 97.
- NNDC, 2017 <http://www.nndc.bnl.gov/nudat2/index_dec.jsp>.
- Otuka, N., Lalremruata, B., Khandaker, M.U., Usman, A.R., Punte, L.R.M., 2017. Uncertainty propagation in activation cross section measurements. *Radiat. Phys. Chem.* <https://doi.org/10.1016/j.radphyschem.2017.01.0133>.
- Petö, G., Milligy, Z., Hunyadi, L., 1967. Radiative capture cross section for 3 MeV neutrons <[http://dx.doi.org/10.1016/0022-3107\(67\)90089-5](http://dx.doi.org/10.1016/0022-3107(67)90089-5)>.
- Poenitz, W.P., 1982. Conference: Argonne National Laboratory report series, Fast-Neutron Capture-Cross-Section Measurements With The Argonne National Laboratory Large-Liquid- Scintillator Tank, Vol. 4, No. 83, p. 239.
- Poppe, C.H., Anderson, J.D., Davis, J.C., Grimes, S.M., Wong, C., 1976. Cross section for the $^7\text{Li}(p, n)^7\text{Be}$ reaction between 4.2 and 26 MeV. *Phys. Rev. C* 14, 438.
- Rigaud, F., Irigaray, J.L., Petit, G.Y., Saporetto, F., 1971. Spectra of high-energy photons following the capture of 14 MeV neutrons by ^{133}Cs , ^{139}La , Ce and ^{159}Tb <[http://dx.doi.org/10.1016/0375-9474\(71\)90936-5](http://dx.doi.org/10.1016/0375-9474(71)90936-5)>.
- Rosman, K.J.R., Taylor, P.D.P., 1998. Isotopic compositions of the elements 1997. *Pure Appl. Chem.* 70, 217.
- Shivashankar, B.S., Ganesan, S., Naik, H., Suryanarayan, S.V., Nair, Sreekumaran, N., Manjunathan, Prasad, K., 2015. Measurement and covariance analysis of reaction cross sections for $^{58}\text{Ni}(n,p)^{58}\text{Co}$ relative to cross section for formation of Zr-97 fission product in neutron-induced fission of Th-232 and U-238 at effective neutron energies $E_n = 5.89, 10.11, \text{ and } 15.87$ MeV. *NSE* 179 (4), 423–433.
- Smith, D.L., 2005. Corrections for Low Energy Neutrons by Spectral Indexing, Retrieved from <<https://www.oecdnea.org/science/docs/2005/nsc-wpec-doc2005-357.pdf>>.
- Uddin, M.S., Sudar, S., Hossain, S.M., Khan, R., Zulquarnain, M.A., Qaim, S.M., 2013. Fast neutron spectrum unfolding of a TRIGA Mark II reactor and measurement of spectrum-averaged cross sections: integral tests of differential cross sections of neutron threshold reactions. *Radiochim. Acta* 101, 613.
- Voignier, J., Joly, S., Grenier, G., 2017. Capture Cross Sections and Gamma-Ray Spectra from the Interaction of 0.5- to 3.0-MeV Neutrons with Nuclei in the Mass Range $A = 45$ to 238. <<http://dx.doi.org/10.13182/NSE91-92N>>.
- Yunshan, Mu, Yexiang, Li, Shiming, Wang, Zhengyu, Xiang, Haishan, Xu, 1988. Measurements of the fast neutron radiative capture cross sections of natural Terbium and Hafnium. *J. Chin. J. Nucl. Phys. (Beijing)* 10 (3) (233 NSR: 1988 MU17).